The Structure of the Route to the Period-three Orbit in the Collatz Map

Weicheng Fu[1,2,3*] and Yisen Wang[3†]
[1] *Department of Physics, Tianshui Normal University, Tianshui 741000, Gansu, China*
[2] *Key Laboratory of Atomic and Molecular Physics & Functional Material of Gansu Province, College of Physics and Electronic Engineering, Northwest Normal University, Lanzhou 730070, China*
[3] *Lanzhou Center for Theoretical Physics, Key Laboratory of Theoretical Physics of Gansu Province, and Key Laboratory of Quantum Theory and Applications of MoE, Lanzhou University, Lanzhou, Gansu 730000, China*

(Dated: December 12, 2024)

This study examines the Collatz map from the perspective of nonlinear dynamics. By expressing integers in terms of Sharkovsky's ordering, we show that it is sufficient to consider only odd initial values for analyzing the iterations. We introduce the concept of "direction phases" to classify the iterations into upward and downward phases, and define a recursive function family F_s based on the number of upward phases. A logarithmic relationship between iteration time and initial values is established, demonstrating that the Collatz map converges to the period-three orbit after a finite number of iterations. We also identify attraction domains with power-law distributions and find that odd numbers classified by upward phases follow a Gamma distribution. Finally, we show that the Collatz map is equivalent to a shift map in binary, and that the ergodicity of the shift map ensures the Collatz map will inevitably evolve onto its attractors, providing theoretical support for the Collatz conjecture. This work offers valuable insights for the study of discrete dynamical systems and related problems in number theory.

I. INTRODUCTION

In both nature and engineering, we frequently encounter dynamic systems with complex and variable behavior, ranging from simple periodic oscillations to unpredictable chaotic phenomena [1–6]. Nonlinear dynamics, as a field dedicated to studying the behaviors of these complex systems, offers a framework for understanding and predicting their dynamic evolution [7]. Discrete dynamical systems, which describe the evolution of system states through iteration, are useful for modeling many practical problems, such as population dynamics, digital signal processing, and periodic phenomena in economics [8]. These systems are typically defined by a set of difference equations, and their iterative behavior can exhibit rich dynamics, including periodicity, chaos, bifurcations, and fractal structures [9–11]. In particular, due to their theoretical importance and practical applications, discrete dynamical systems have become a key area of research for nonlinear dynamics [12–16].

In the study of nonlinear dynamics, Sharkovsky's theorem [17, 18] and Li-Yorke's theorem [19] are two landmark achievements. Sharkovsky's theorem reveals the coexistence of different periodic solutions in one-dimensional discrete mapping systems and establishes an ordering of these solutions, known as Sharkovsky ordering [20]. This ordering shows that the existence of some periodic solutions can be derived from others, and the existence of a period-three solution implies the existence of solutions for all integer periods. Li-Yorke's theorem, famously summarized as "Period three implies chaos" both rediscovered a key idea from Sharkovsky's theorem and provided a formal definition of chaos [19]. It demonstrates that chaotic systems are highly sensitive to initial conditions, meaning small differences in initial states can lead to vastly different outcomes, making long-term predictions difficult [21, 22]. The discovery of deterministic chaos profoundly challenges the traditional notions of certainty and predictability, revealing that certainty does not equate to predictability. This insight prompts scientists to reconsider the nature of natural laws. For example, classical science, represented by Newtonian mechanics, struggles to address nonlinear systems, while chaos theory offers a new perspective for understanding such complex phenomena [23–25]. It should be noted that the "Period three implies chaos" here only applies to the continuous map of the interval to the interval itself, and does not necessarily hold true for the discrete map.

In this study, we treat the Collatz map as a discrete dynamical system and investigate its statistical behavior using methods and concepts from nonlinear dynamics [26]. The Collatz map, also known as the Collatz conjecture or the $3X+1$ problem, is one of the most famous unsolved problems in mathematics, primarily due to its deceptively simple formulation and unresolved status [27] (also see references therein). The conjecture states that for any positive integer X, repeatedly applying the transformation multiplying by 3 and adding 1 when X is odd, or dividing by 2 when X is even will eventually lead to

* fuweicheng@tsnu.edu.cn
† wys@lzu.edu.cn

the cycle $\{4, 2, 1\}$.

Substantial progress has been made in understanding the statistical properties and probabilistic behavior of Collatz orbits, providing heuristic evidence supporting the conjecture. Pioneering work by Crandall laid the groundwork by establishing constraints on the behavior of the transformation and linking it to Diophantine equations [28]. Later studies, such as those by Krasikov, used statistical methods to approximate the number of integers satisfying the conjecture, contributing further to a probabilistic framework for understanding its dynamics [29]. More recently, Tao introduced advanced techniques involving random walks and skew distributions on cyclic groups to analyze the limiting behavior of the sequence for almost all integers, in the sense of logarithmic density, bringing us closer to validating the conjecture for most integers [30].

In fact, if it can be proven that the three-period orbit $\{4, 2, 1\}$ is the only one, and that the number of iterations required to reach this cycle from any integer is finite (rather than divergent), the Collatz conjecture would become the Collatz theorem. Unfortunately, despite significant computational verification for large numbers and various partial results, a general proof remains elusive.

In this study, we represent integers using Sharkovsky's ordering and demonstrate that analyzing the iterations of the Collatz map only requires considering odd initial values. We introduce the concept of direction phases to classify iterations into upward and downward phases and define a recursive function family F_s based on the number of upward phases. A logarithmic relationship between iteration time and initial values is established, showing that the Collatz map converges to the period-three orbit after a finite number of iterations.

Additionally, we identify attraction domains that follow power-law distributions and find that odd numbers classified by upward phases approximately follow a Gamma distribution. Finally, we show that the Collatz map is equivalent to a shift map in binary. The ergodicity of the Bernoulli shift map [31] guarantees that the Collatz map will inevitably evolve toward its attractors, providing theoretical support for the Collatz conjecture.

Our research offers insights into the dynamics of discrete systems and their connections to number theory. The paper is organized as follows: Section II introduces the Collatz map, Section III presents the theoretical analysis, Section IV provides our numerical results, and Section V concludes with a discussion.

II. THE COLLATZ MAP

The Collatz map reads as

$$X_{n+1} = \begin{cases} \frac{X_n}{2}, & \mod (X_n, 2) = 0; \\ 3X_n + 1, & \mod (X_n, 2) \neq 0, \end{cases} \tag{1}$$

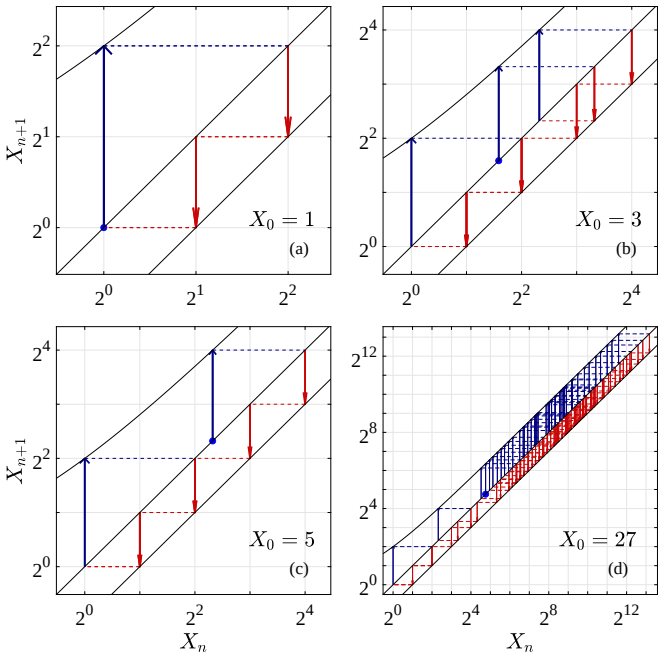

FIG. 1. A cobweb plot for orbits of different X_0 in log-log scale.

where X_n is a positive integer, viz. $X_n \in \mathbb{Z}^+$. For brevity, the map is abbreviated as $X_n = M^n(X_0)$. The Collatz conjecture posits that

$$\lim_{n\to\infty} M^n(X_0) = \{4, 2, 1\} \quad \text{for } \forall X_0 \in \mathbb{Z}^+, \tag{2}$$

namely, after several iterations the map M will evolve into the period-three orbit of $\{4, 2, 1\}$ from any positive integer.

To facilitate further theoretical analysis, we introduce the concept of direction phase order [32]. Specifically, we define $P(n) = 1$ for $X_{n+1} - X_n > 0$ (the up phase, denoted as $P_\uparrow$) and $P(n) = -1$ for $X_{n+1} - X_n < 0$ (the down phase, denoted as $P_\downarrow$). The number of up and down phases before entering the period-three orbit $\{1, 4, 2\}$ are denoted as $N_\uparrow$ and $N_\downarrow$, respectively.

For example, Fig. 1(a) shows a cobweb plot for the orbit starting at $X_0 = 1$. The trajectory follows a period-three cycle, i.e., $M^3(1) = 1$, consisting of one up phase (blue up arrow) and two down phases (red down arrows). Figure 1(b) presents the results for $X_0 = 3$, where the map enters the periodic orbit $\{1, 4, 2\}$ after 7 iterations, i.e., $M^7(3) = 1$.

From Figs. 1(b)-(d), we observe the following values for $N_\uparrow$ and $N_\downarrow$: For $X_0 = 3$, $N_\uparrow = 2$ and $N_\downarrow = 5$. For $X_0 = 5$, $N_\uparrow = 1$ and $N_\downarrow = 4$. For $X_0 = 27$, $N_\uparrow = 41$ and $N_\downarrow = 70$. Note that $N_\uparrow$ and $N_\downarrow$ represent the total number of odd and even numbers in the sequence from X_0 (where $X_0 \neq 1$) to 2, respectively. The total number of iterations is given by:

$$N = N_\uparrow + N_\downarrow, \tag{3}$$

which implies $M^N(X_0) = 1$.

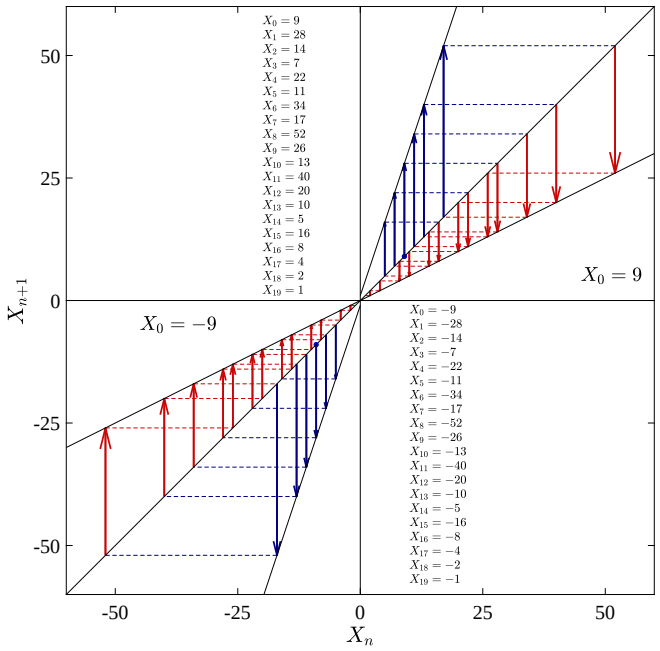

FIG. 2. A cobweb plot for orbits of $X_0 = \pm 9$.

In fact, if we multiply both sides of Eq. (1) by -1, the equation still holds. Therefore, the Collatz map can be generalized as follows:

$$X_{n+1} = \begin{cases} \frac{X_n}{2} & \text{if } X_n \text{ is even;} \\ 3X_n + \text{sgn}(X_n) & \text{if } X_n \text{ is odd,} \end{cases} \tag{4}$$

where $X_n \in \mathbb{Z} = \mathbb{Z}^- \cup \{0\} \cup \mathbb{Z}^+$, and $\text{sgn}(x)$ is the sign function. The Collatz conjecture is then rewritten as:

$$\lim_{n\to\infty} M^n(X_0) = \begin{cases} \{-1,-4,-2\}, & \text{if } X_0 \in \mathbb{Z}^-; \\ \{0\}, & \text{if } X_0 = 0; \\ \{1,4,2\}, & \text{if } X_0 \in \mathbb{Z}^+. \end{cases} \tag{5}$$

In Fig. 2, we show a cobweb plot for the orbits of $X_0 = \pm 9$, which reveals that the two iterated orbits are symmetric about the origin and eventually converge to ± 1, respectively. Therefore, in this study, we will focus on the case where $X_0 \in \mathbb{Z}^+$. With these concepts in place, we will now proceed with a detailed theoretical analysis.

III. THEORETICAL ANALYSIS

We define two infinite-length row vectors:

$$\boldsymbol{B} = [2^0, 2^1, 2^2, \ldots, 2^m, \ldots]1, \infty, \tag{6}$$

and

$$\boldsymbol{O} = [3, 5, 7, \ldots, 2n+1, \ldots]1, \infty, \tag{7}$$

along with an infinite-dimensional matrix $\boldsymbol{D} = \boldsymbol{B}^{\mathrm{T}}\boldsymbol{O}$, which is given by:

$$\boldsymbol{D} = \begin{bmatrix} 3 & 5 & \ldots & (2n+1)\cdot 2^0 & \ldots \\ 3\cdot 2 & 5\cdot 2 & \ldots & (2n+1)\cdot 2^1 & \ldots \\ 3\cdot 2^2 & 5\cdot 2^2 & \ldots & (2n+1)\cdot 2^2 & \ldots \\ \vdots & \vdots & \ldots & \vdots & \vdots \\ 3\cdot 2^m & 5\cdot 2^m & \ldots & (2n+1)\cdot 2^m & \ldots \\ \vdots & \vdots & \ldots & \vdots & \vdots \end{bmatrix}. \tag{8}$$

Suppose the elements in the vectors $\boldsymbol{B}$ and $\boldsymbol{O}$, as well as the matrix $\boldsymbol{D}$, form the sets $\mathbb{B}$, $\mathbb{O}$, and $\mathbb{D}$, respectively. It is clear that all elements of the sets $\mathbb{D}$ and $\mathbb{B}$ follow the Sharkovsky ordering [17, 18, 20], meaning that $\mathbb{D} \cup \mathbb{B} \equiv \mathbb{Z}^+$.

Notably, if $X_0 = 2^m \in \mathbb{B}$, then $X_m = M^m(X_0) = 1$, corresponding to $N_\uparrow = 0$ and $N = N_\downarrow = m$, which represents a simple and trivial trajectory. On the other hand, if $X_0 = (2n+1)\cdot 2^m \in \mathbb{D}$, then $X_m = M^m(X_0) = 2n+1 \in \mathbb{O}$. Therefore, for the Collatz map, we only need to consider the case where $X_0 \in \mathbb{O}$.

A. Estimation of iterative times

Assuming that $X_0 \in \mathbb{O}$ and $N_\uparrow = 1$, i.e., $X_1 = 2^m \in \mathbb{B}$. In this case, we have the following equation:

$$X_0 = F_1(m) = \frac{2^m - 1}{3} \in \mathbb{O}, \tag{9}$$

where $m > 2$, and F_1 satisfies the recursion relation:

$$F_1(m) = 2^{m-2} + F_1(m-2). \tag{10}$$

It is easy to prove that $X_0 = F_1(m) \in \mathbb{O}$ if and only if $m = 2p$ is an even number, where $p \in \mathbb{Z}^+$. In contrast, if m is odd, then F_1 is a fraction, i.e., $F_1 \notin \mathbb{O}$. For brevity, we define:

$$F_1(p) = \frac{2^{2p} - 1}{3} = \frac{4^p - 1}{3}. \tag{11}$$

Note that $F_1(1) = 1 \in \mathbb{B}$ when $p = 1$. However, for the case $X_0 = F_1(p) \in \mathbb{O}$, assuming $p \geq 2$, we then obtain the following recursion formula:

$$F_1(p) = 4^{p-1} + F_1(p-1). \tag{12}$$

Additionally, we have $N_\downarrow = 2p = \log_2(3X_0 + 1)$ for $X_0 = F_1(p)$. Therefore, the total number of iterations for convergence, when $N_\uparrow = 1$, is:

$$N_1 = N_\uparrow + N_\downarrow = 1 + 2p = 1 + \log_2(3X_0 + 1). \tag{13}$$

Next, suppose $X_0 \in \mathbb{O}$ and $N_\uparrow = 2$. We then have:

$$X_0 = F_2(p, k_1) = \frac{2^{k_1} F_1(p) - 1}{3} \in \mathbb{O}, \tag{14}$$

where $k_1 \in \mathbb{Z}^+$. It is evident that:

$$F_2(p,k_1) = F_2(p,k_1-2) + 2^{k_1-2}F_1(p), \tag{15}$$

and

$$k_1 = \log_2(3X_0+1) - \log_2(X_0). \tag{16}$$

Thus, the total number of iterations at $N_\uparrow = 2$ is:

$$N_2 = 2 + 2p + k_1 = 2 + 2\log_2(3X_0+1) - \log_2(X_0). \tag{17}$$

Similarly, for $N_\uparrow = 3$, we have:

$$X_0 = F_3(p,k_2) = \frac{2^{k_2}F_2(p,k_1)-1}{3} \in \mathbb{O}, \tag{18}$$

where $k_2 \in \mathbb{Z}^+$, and

$$k_2 = \log_2(3X_0+1) - \log_2(X_0). \tag{19}$$

Furthermore, the function F_3 satisfies:

$$F_3(p,k_2) = F_3(p,k_2-2) + 2^{k_2-2}F_2(p,k_1). \tag{20}$$

Thus, the total number of iterations at $N_\uparrow = 3$ is:

$$\begin{aligned} N_3 &= 3 + 2p + k_1 + k_2 \\ &= 3 + 3\log_2(3X_0+1) - 2\log_2(X_0). \end{aligned} \tag{21}$$

Likewise, for the case of $N_\uparrow = s$, we define:

$$X_0 = F_s(p,k_{s-1}) = \frac{2^{k_{s-1}}F_{s-1}(p,k_{s-2})-1}{3} \in \mathbb{O}, \tag{22}$$

where $k_{s-1} \in \mathbb{Z}^+$, and

$$k_{s-1} = \log_2(3X_0+1) - \log_2(X_0). \tag{23}$$

The function F_s follows the recursion relation:

$$F_s(p,k_{s-1}) = F_s(p,k_{s-1}-2) + 2^{k_{s-1}-2}F_{s-1}(p,k_{s-2}). \tag{24}$$

The total number of iterations at $N_\uparrow = s$ is given by:

$$\begin{aligned} N_s &= N_\uparrow + N_\downarrow = s + 2p + \sum_{j=1}^{s-1} k_j \\ &= s + s\log_2(3X_0+1) - (s-1)\log_2(X_0) \\ &= s\left[1 + \log_2\left(3 + \frac{1}{X_0}\right)\right] + \log_2(X_0), \end{aligned} \tag{25}$$

which is one of our main theoretical results.

In fact, the function F_s can be expressed in an explicit form. For example:

$$F_4(p,k_3) = \frac{2^{k_3}\left\{\frac{2^{k_2}\left[\frac{2^{k_1}\left(\frac{4^p-1}{3}\right)-1}{3}\right]-1}{3}\right\} - 1}{3} = \frac{2^{2p+k_1+k_2+k_3}}{3^4} - \frac{2^{k_1+k_2+k_3}}{3^4} - \frac{2^{k_2+k_3}}{3^3} - \frac{2^{k_3}}{3^2} - \frac{1}{3}. \tag{26}$$

This clearly shows that the powers of 2 are successively decreasing positive integers. Therefore, F_s can be abbreviated as:

$$\begin{aligned} F_s &= \boldsymbol{a}_s \cdot \boldsymbol{b}_s, \\ \boldsymbol{a}_s &= \frac{1}{3^s}[1, -3^0, -3^1, \ldots, -3^{s-3}, -3^{s-2}, -3^{s-1}], \\ \boldsymbol{b}_s &= [2^{k_s}, 2^{k_{s-1}}, 2^{k_{s-2}}, \ldots, 2^{k_2}, 2^{k_1}, 2^0], \end{aligned} \tag{27}$$

where $\boldsymbol{a}_s \cdot \boldsymbol{b}_s$ denotes the inner product of the two vectors, and the integers k_s satisfy the condition $k_s > k_{s-1} > k_{s-2} > \cdots > k_1 \geq 1$. A similar function was presented in Ref. [27]. Note that if $X_0 = F_s$, then $N_\downarrow = k_s$, resulting in $N_s = s + k_s$.

Clearly, from Eq. (25), we see that N_s increases logarithmically as X_0 increases. In fact, the behavior of N_s with respect to X_0 is more important than the specific magnitude of N_s. For example, when $X_0 = 2^m \in \mathbb{B}$ and $m \to \infty$, we have $N_0 = m \to \infty$. However, we can also observe that

$$\lim_{m\to\infty} \frac{N_0}{X_0} = \lim_{m\to\infty} \frac{m}{2^m} = 0, \tag{28}$$

which indicates that the number of iterations required to reach convergence remains finite relative to X_0.

For a fixed value of s, Eq. (25) leads to the following result:

$$\lim_{X_0\to\infty} \frac{N_s}{X_0} = \lim_{X_0\to\infty} \frac{1}{X_0 \ln 2} = 0, \tag{29}$$

which suggests that the Collatz conjecture holds for $X_0 \in \mathbb{F}$, where $\mathbb{F}$ is the set of all integers generated by the family of functions F_s. If $\mathbb{F} \equiv \mathbb{O} \cup \{1\}$, that is, if all odd numbers can be generated by F_s, then the Collatz conjecture is valid for all positive integers.

Interestingly, the results obtained here, based on deterministic rules, are qualitatively consistent with the conclusion by Tao—*"almost all orbits of the Collatz map attain almost bounded values"*—which was derived using probability theory [30].

B. Definition of attraction domain

From the above theoretical analysis, it is evident that the function F_s exhibits a self-similar structure. Regardless of the value of s, it always enters the decay orbit $X_{N_s-2p} = 4^p \in \mathbb{B}$. In other words, $X_{N_s-2p-1} = \frac{4^p-1}{3} \in \mathbb{O}$ serves as the entry point for X_0 to enter the periodic orbit. Specifically, for $X_0 \in \mathbb{O}$, $X^p = F_1(p) = \frac{4^p-1}{3}$ acts like a black hole: once X^p appears in the iteration sequence, the next iteration will inevitably map $M(X^p) \in \mathbb{B}$, causing the map to enter the periodic orbit unidirectionally.

We therefore *define* the set of $\{X_0\}$ with the same p-value as the *attraction domain* of p. For convenience, we refer to X^p as an attractor. In the following, we will

	2^{16}	2^{15}	2^{14}	2^{13}	2^{12}	2^{11}	2^{10}	2^{9}	2^{8}	2^{7}	2^{6}	2^{5}	2^{4}	2^{3}	2^{2}	2^{1}	2^{0}
p=2	0	0	0	0	0	0	0	0	0	0	0	0	0	0	1	0	1
p=3	0	0	0	0	0	0	0	0	0	0	0	0	1	0	1	0	1
p=4	0	0	0	0	0	0	0	0	0	0	1	0	1	0	1	0	1
p=5	0	0	0	0	0	0	0	0	1	0	1	0	1	0	1	0	1
p=6	0	0	0	0	0	0	1	0	1	0	1	0	1	0	1	0	1
p=7	0	0	0	0	1	0	1	0	1	0	1	0	1	0	1	0	1
p=8	0	0	1	0	1	0	1	0	1	0	1	0	1	0	1	0	1
p=9	1	0	1	0	1	0	1	0	1	0	1	0	1	0	1	0	1

FIG. 3. The binary representations of $X^p = (4^p - 1)/3$ =5, 21, 85, 341, 1365, 5461, 21845, 87381 for $p = 2, 3, \ldots, 9$.

investigate the properties of the attraction domain by analyzing the behavior of F_s.

Note that when $p = 1$, F_s and F_1 exhibit exactly the same behavior, which is a trivial case. Thus, we focus on cases where $p \geq 2$. To begin, we examine the properties of $F_2(p, k_1)$. Clearly, if we know the values of $F_2(p, 1)$ and $F_2(p, 2)$, we can compute all subsequent values of $F_2(p, k_1)$ using the recursion relation.

From Eq. (15), we have the following relations:

$$F_2(p + 3, 1) = 7 \cdot 2^{2p+1} + F_2(p, 1), \tag{30}$$

and

$$F_2(p + 3, 2) = 7 \cdot 2^{2p+2} + F_2(p, 2). \tag{31}$$

Additionally, the specific values are:

$$F_2(1, 1) = \frac{1}{3}, \quad F_2(2, 1) = 3, \quad F_2(3, 1) = \frac{41}{3},$$
$$F_2(1, 2) = 1, \quad F_2(2, 2) = \frac{19}{3}, \quad F_2(3, 2) = \frac{83}{3}.$$

Therefore, $F_2(p, k_1)$ is an odd number when $p = 2 + 3m$ and $k_1 = 2n - 1$, or when $p = 4 + 3m$ and $k_1 = 2n$, where $m \in \mathbb{Z}$ and $n \in \mathbb{Z}^+$. However, $F_2(p, k_1)$ is a fraction when $p = 3n$, which implies that only one number, namely $X_0 = X^p$, lies in the attraction domain of $p = 3n$.

C. The scheme of like-Bernoulli shift

Assuming that $X_0 = 2n + 1 \in \mathbb{O}$, we have

$$X_1 = M(X_0) = X_0 + 2X_0 + 1, \tag{32}$$

and

$$X_2 = M(X_1) = 2^{-1}X_1 = M^2(X_0), \tag{33}$$

where X_1 must be an even number, as shown in Fig. 4. Suppose that $2^{m-1} < X_0 < 2^m$, then, X_0 can be written as

$$X_0 = 2^{m-1} + \sum_{j=1}^{m-2} c_j 2^j + 2^0, \tag{34}$$

State	2^m	2^{m-1}	2^{m-2}	…	2^2	2^1	2^0
X_0		1	c_{m-2}	…	c_2	c_1	1
$2X_0$+1	1	c_{m-2}	…	c_2	c_1	1	1
X_1	1	1+c_{m-2}	c_{m-2}+c_{m-3}	…	c_2+c_1+1	c_1	0
X_2	…	…	…	…	…	…	c_1

FIG. 4. Demonstration of iteration process in binary system which looks like a scheme of Bernoulli shift.

where c_j takes the values 0 or 1, and $c_0 = c_{m-1} = 1$. Figure 3 shows the binary representation of the attractor X^p for $p = 2, 3, \ldots, 9$. It can be observed that the binary representation of the attractor exhibits a high degree of self-similarity.

The Collatz map can be clearly demonstrated through the process shown in Fig. 4. Specifically, the operation of multiplying by 2 and then adding 1, i.e., $2X_0 + 1$, is equivalent to shifting the binary representation of X_0 one bit to the left and adding 1 at the end. On the other hand, $X_1 = 3X_0 + 1$ is equivalent to adding the binary coefficients of X_0 to those of $2X_0 + 1$. When the sum of coefficients reaches 2, a carry is required to the next higher bit, similar to carrying over in decimal addition when the sum reaches 10. Specifically, if $c_2' = (c_2+c_1+1) \geq 2$, then $c_2' = (c_2+c_1+1)-2$, and this results in $c_3' = c_3 + c_2 + 1$, where c_j' are the coefficients of X_1. This carry operation is repeated for all other positions as well.

We see that the operation $M^2(X_0)$ is equivalent to moving c_1 of X_0 to the position of c_0 in X_2, while the coefficients in other positions are updated by adding the corresponding coefficients. In this case, $N_\uparrow = 1$. If $c_1 = 1$, then $N_\uparrow = 1 + 1$, and the shift operation for X_2 is similar to that for X_0. However, if $c_1 = 0$, then c_2' is shifted to the position of 2^0, i.e., $c_0'' = c_2'$.

Statistically, the shift operation tends to move to the right, since the values of c_1 (0 or 1) are equally probable. Furthermore, from the perspective of the ergodicity of a Bernoulli symbol sequence, after a finite number of shift operations, the state of X^p will eventually appear (see Fig. 3). In other words, the ergodicity of the Bernoulli shift guarantees the validity of the Collatz conjecture.

IV. NUMERICAL VERIFICATION

Based on the theoretical analysis above, we only need to consider the case where $X_0 \in \mathbb{O}$ in the numerical simulations. Although the set $\mathbb{O}$ contains an infinite number of elements, in practical purposes, we restrict X_0 to finite intervals in the simulations and conduct statistical analysis. For example, we choose $X_0 \in \{3, 5, \ldots, 2n_{\max} + 1\}$ and then count how many numbers belong to the attraction domain p.

Figure 5(a) shows the count $\mathcal{N}(p)$ as a function of p for various values of $n_{\max}$. We observe that, regardless of the

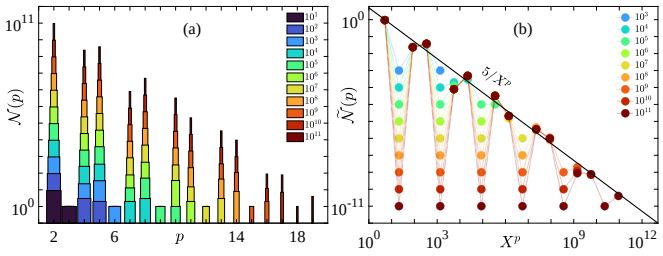

FIG. 5. (a) Histograms of number $\mathcal{N}(p)$ in different attraction domains p within a given range of $X_0 \in \{3, 5, \ldots, 2n_{\max}+1\}$. The legend shows the value of $n_{\max}$. (b) Same as the panel (a) but in normalized form $\widetilde{\mathcal{N}}(p) = \mathcal{N}(p)/n_{\max}$ and the horizontal axis has been changed to $X^p = F_1(p)$. The solid line is drawn for reference.

value of $n_{\max}$, $\mathcal{N}(p=2)$ is always the largest. Additionally, $\mathcal{N}(p) = 1$ when $\mathrm{mod}(p, 3) \equiv 0$, which is consistent with the theoretical analysis presented in subsection B of Sec. III.

Figure 5(b) plots the normalized count $\widetilde{\mathcal{N}} = \mathcal{N}/n_{\max}$, which represents the percentage of numbers in each attraction domain. It is noteworthy that, except for numbers where $\mathrm{mod}(p, 3) \equiv 0$, $\widetilde{\mathcal{N}}(p) \propto 1/X^p$, as shown by the black reference line. For larger values of $n_{\max}$, $\widetilde{\mathcal{N}}(p=2) \approx 93.77\%$, as detailed in Tab. I.

In principle, the value of p can extend to infinity, so it is reasonable to expect that the numerical distribution in Tab. I will resemble the form of an upper triangular matrix. Of course, to observe non-zero values for larger p, a larger $n_{\max}$ is required. Based on the data, it is reasonable to infer that as $p \to \infty$ and $n_{\max} \to \infty$, the following holds: $\widetilde{\mathcal{N}}(p=2) \approx 93.77\%$, $\widetilde{\mathcal{N}}(p=4) \approx 2.37\%$, and $\widetilde{\mathcal{N}}(p=5) \approx 3.79\%$. In other words, $\widetilde{\mathcal{N}}(p=2,4,5) \approx 99.93\%$ remains essentially unchanged, and increasing p and $n_{\max}$ only affects the significant digits of the decimal point. It is clear that the size of the attraction domain follows a power-law distribution.

To visualize the distribution of attraction domains more intuitively, we used the Ulam spiral method [33] to plot graphs for different intervals. The results, shown in Fig. 6, reveal a highly intricate structure. When viewing the animation through a moving window, we observe rich self-similarity patterns.

In Fig. 7(a), the ratio $N_\downarrow/N_\uparrow$ as a function of X_0 is shown. Different colored points represent numbers belonging to different attraction domains. The solid lines correspond to theoretical predictions given by Eq. (25). It can be seen that the theoretical and numerical results align very well. Additionally, the ratio approaches $\log_2(3) \approx 1.585$ as $N_\uparrow$ increases, as indicated by the purple horizontal dashed line.

Figure 7(b) shows the dependence of the total number of iterations, $N = N_\downarrow + N_\uparrow$, on X_0. It is noteworthy that as X_0 increases, N grows slowly. The numerical results are fully consistent with the theoretical predictions, as shown by the solid lines from Eq. (25). This supports

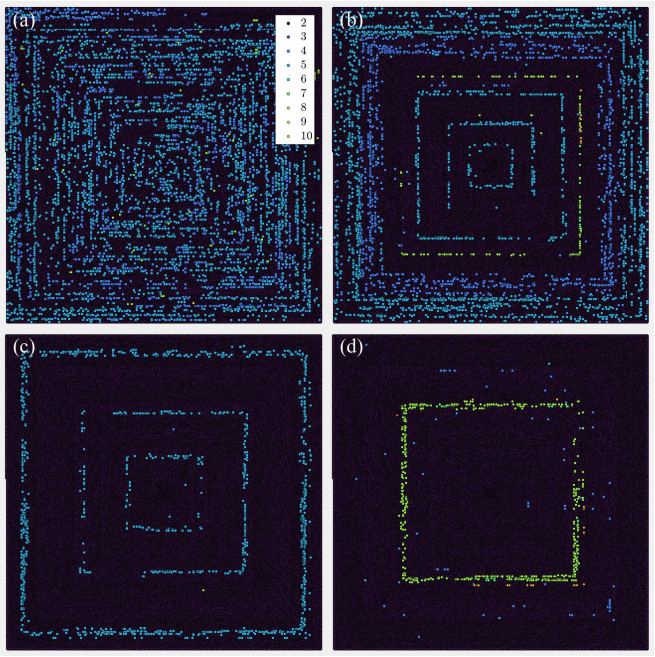

FIG. 6. The distribution of attraction domains of different intervals using the Ulam spiral drawing method. Each panel plots 10^5 points and $X_0 = 2n+1$. (a) $n \in [1, 2, \ldots, 10^5]$. (b) $n \in [103 \times 10^5 + 1, \ldots, 104 \times 10^5]$. (c) $n \in [401 \times 10^5 + 1, \ldots, 402 \times 10^5]$. (d) $n \in [644 \times 10^5 + 1, \ldots, 645 \times 10^5]$.

the conclusion that the number of iterations required for convergence is indeed a finite value relative to X_0, confirmed Eqs. (28) and (29).

Furthermore, in Fig. 7(b), the purple crossed dotted line marks the upper boundary of the region, which consists of the points with the smallest X_0 for a given $N_\uparrow$. We observe that the boundaries of the attraction domains for different p resemble coastlines and exhibit a high degree of similarity. Notably, the distribution of the attraction domain for $p = 2$ nearly covers the entire range of the calculated interval, which is consistent with the statistical results presented in Fig. 5. Specifically, the numbers on the upper boundary all belong to the attraction domain of $p = 2$.

To investigate the properties of the numbers at the upper boundary marked in Fig. 7(b) in more detail, we present the behavior of these numbers over a broader range in Fig. 8. The abscissa (X_0) and ordinate (N) of the boundary points as functions of $N_\uparrow$ are shown in Figs. 8(a)-(c). Figure 8(a) demonstrates that X_0 increases nearly in a stretched exponential manner with $N_\uparrow$ (see the magenta dashed curve), which is faster than a power-law growth (black dashed line), but slower than exponential growth (black dashed line in the inset). Figure 8(b) provides a clearer depiction of how X_0 increases with $N_\uparrow$. Additionally, a self-similarity fractal structure, reminiscent of a coastline, is observed in the distribution of X_0.

Figure 8(c) shows the dependence of N on $N_\uparrow$, where N

TABLE I. Statistics of numbers in different attraction domains p within a given range of $X_0 \in [3, 5, \ldots, 2n+1]$.

p	$n = 10^1$	10^2	10^3	10^4	10^5	10^6	10^7	10^8	10^9	10^{10}	10^{11}
2	9	94	940	9395	93679	938003	9378361	93772537	937676531	9377184597	93774780663
3	1	1	1	1	1	1	1	1	1	1	1
4	0	3	23	255	2412	23743	237828	2373777	23761165	237454856	2373306190
5	0	2	35	343	3842	37687	377838	3793838	37961580	379374692	3792124780
6	0	0	1	1	1	1	1	1	1	1	1
7	0	0	0	2	13	78	830	8098	80062	796409	7937609
8	0	0	0	3	50	448	4810	48229	485728	4843192	48398337
9	0	0	0	0	1	1	1	1	1	1	1
10	0	0	0	0	1	36	311	3253	32329	320937	3199254
11	0	0	0	0	0	2	15	212	2127	20883	206700
12	0	0	0	0	0	0	1	1	1	1	1
13	0	0	0	0	0	0	3	44	363	3419	34128
14	0	0	0	0	0	0	0	8	108	974	9551
15	0	0	0	0	0	0	0	0	1	1	1
16	0	0	0	0	0	0	0	0	2	12	88
17	0	0	0	0	0	0	0	0	0	7	78
18	0	0	0	0	0	0	0	0	0	0	1
19	0	0	0	0	0	0	0	0	0	0	4

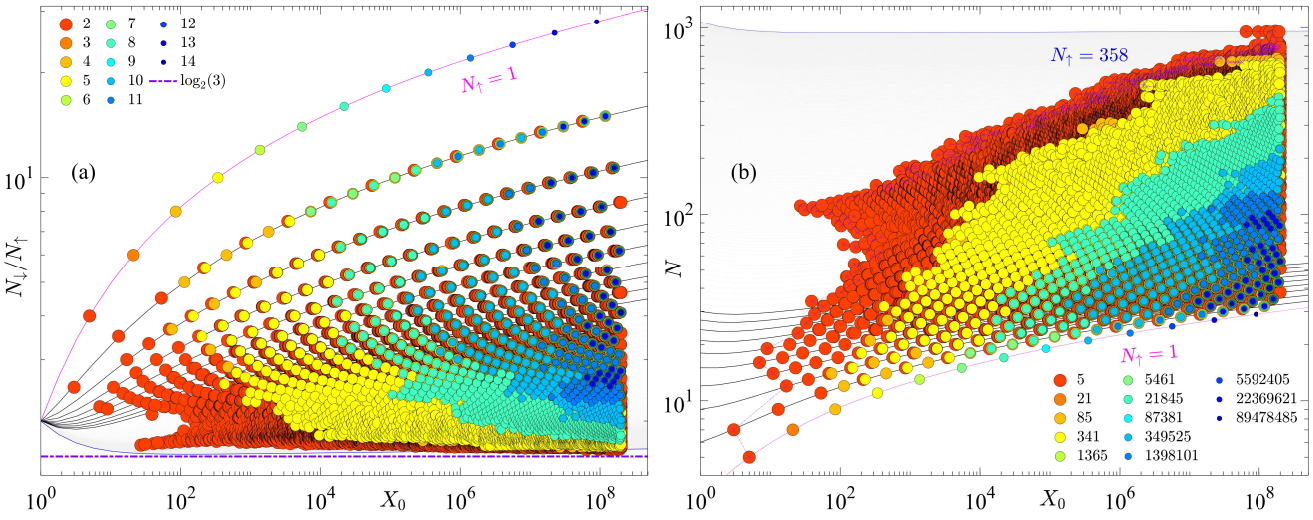

FIG. 7. The dependence of $N_\downarrow/N_\uparrow$ (a) and $N = N_\downarrow + N_\uparrow$ (b) on $X_0 = 2n+1$ for $n = 1, 2, \ldots, 10^8$. Different colored points indicate belonging to different attraction domains p, see the legend in panel (a), while the legend in panel (b) shows the value of $F_1(p)$. The solid lines are the theoretical predictions given by expression (25). The dotted purple line marked by cross in panel (b) gives the upper boundary of the region, which is replotted in Fig. 8(a).

increases approximately linearly with $N_\uparrow$. From Eq. (25), for large X_0, we have $N \approx [1 + \log_2(3)]N_\uparrow$, which agrees with the numerical results shown in Fig. 8(c). Finally, Fig. 8(d) displays the ratio N/X_0 as a function of X_0, where the black line represents the theoretical prediction derived from Eq. (25). It is clear that as $X_0 \to \infty$, $N/X_0 \to 0$, indicating that the number of iterations required to converge to the period-three orbit becomes negligible relative to large X_0. In this sense, the Collatz conjecture holds for all positive integers.

Figure 9 shows the distribution of numbers over $N_\uparrow$ for a given range of $X_0 \in [3, 5, \ldots, 2n_{\max}+1]$. In other words, the height of the histogram represents the proportion of numbers with the same $N_\uparrow$. From Figs. 9(a)-(g), we observe that the distribution approximately follows a Gamma distribution of the form $\rho(x) = \frac{A}{\theta^K \Gamma(K)} x^{K-1} e^{-x/\theta}$ (solid line in each panel). Moreover, the distribution function becomes flatter as $n_{\max}$ increases, as shown by the solid lines in Fig. 9(h).

Figure 10(a) shows the dependence of the parameters of the Gamma distribution function on $n_{\max}$. We observe that $A \simeq 1$ remains constant, K increases as $K \sim \log_{10}(n_{\max})$ with $n_{\max}$, and θ exhibits a slow decay, remaining approximately constant within the range considered. As is known, the mean value of the Gamma distribution is given by $K\theta$, which also increases as $n_{\max}$

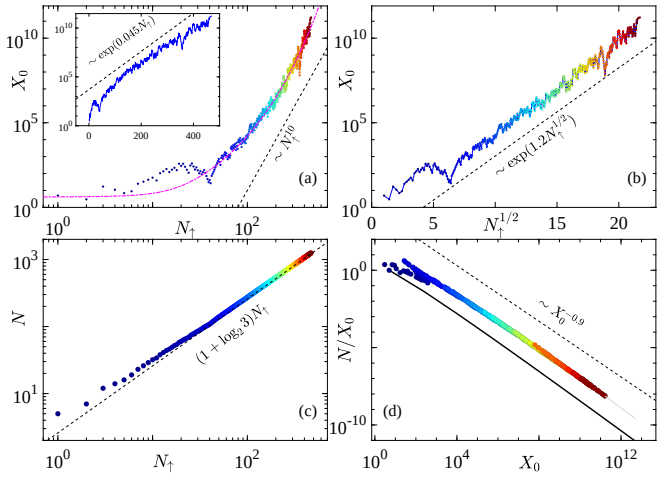

FIG. 8. (a) X_0 of the upper boundary points in Fig. 7(b) as a function of $N_\uparrow$ in log-log scale. The magenta dashed line is a plot of a stretched exponential function $\exp(1.2N_\uparrow^{1/2})/7+4$ for reference. Inset: Same as the main panel but in semi-log scale. (b) Same as the panel (a) but the abscissa is rescaled as $N_\uparrow^{1/2}$. The data in panels (c) and (d) are the same as that in panel (a) but shows in different forms. (c) $N = N_\uparrow + N_\downarrow$ as a function of $N_\uparrow$. (d) The dependence of $N_\uparrow/X_0$ on X_0. The black line is given by formula (25) for $N_\uparrow = 1$. The dashed lines in all panels are plotted for reference.

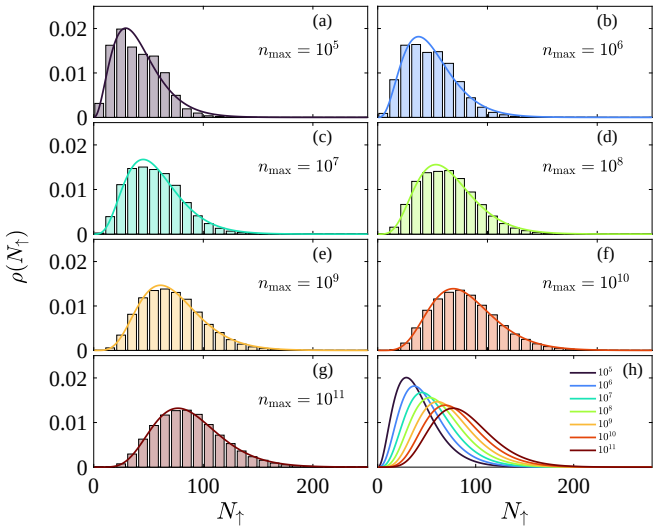

FIG. 9. (a)-(g) The distribution of numbers over $N_\uparrow$ within a given interval of $X_0 \in [3, 5, \ldots, 2n_{\max}+1]$. The solid line is a fitting curve based on the Gamma distribution with the form of $\rho(x) = \frac{A}{\Gamma(K)\theta^K} x^{K-1} e^{-x/\theta}$. (h) Summarize all fitted curves together for comparison.

increases, as shown in Fig. 10(b). This suggests that the mean value of $\overline{N\uparrow} = K\theta \approx 2.54 + 7.79 \log 10(n_{\max})$.

We further calculate the distribution of numbers across different attraction domains p over $N_\uparrow$ within the range $X_0 \in [3, 5, \ldots, 2n_{\max}+1]$, where $n_{\max} = 10^{11}$ is fixed (we have verified that changing the value of $n_{\max}$ produces

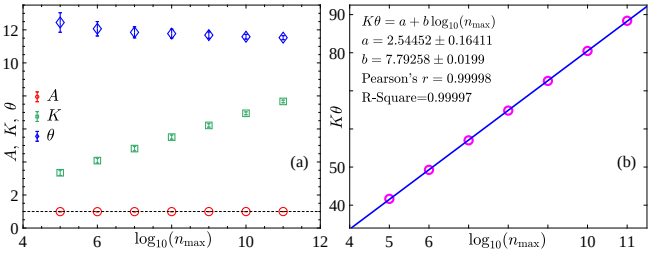

FIG. 10. (a) The fitting parameters of the Gamma distribution function in Fig. 9 as a function of $n_{\max}$. (b) Dependence of the mean value of the Gamma distribution $K\theta$ on $n_{\max}$.

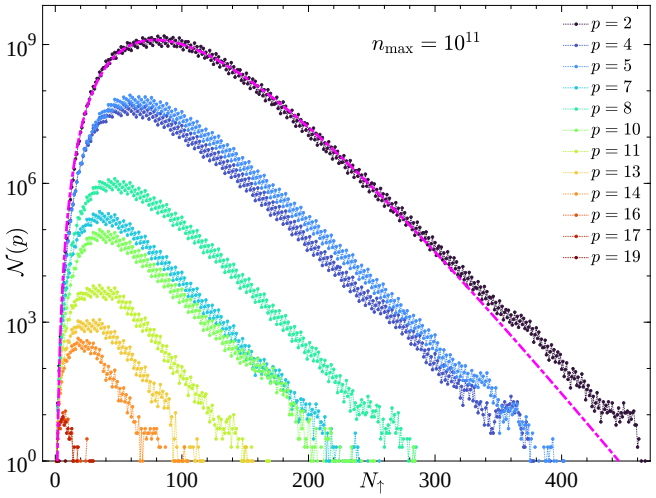

FIG. 11. The count number $\mathcal{N}(p)$ over $N_\uparrow$ within a given interval of $X_0 \in [3, 5, \ldots, 2n_{\max}+1]$ in log-log scale. The magenta dashed line is a fitting curve based on the Gamma distribution.

qualitatively identical results). The numerical results are shown in Fig. 11, where $\mathcal{N}(p)$ represents the number of numbers belonging to the attraction domain p. It is evident that all $\mathcal{N}(p)$ follow a Gamma distribution, with different parameters for each p (see the magenta dashed curve, which nearly covers all points for $p = 2$). Additionally, we observe that the distribution range for $\mathcal{N}(p = 2)$ is the largest among all the values of p, which is consistent with the statistical results presented in Fig. 5.

V. SUMMARY AND DISCUSSIONS

In summary, we have explored the properties of the Collatz map from the perspective of nonlinear dynamical systems. By expressing all positive integers in terms of the Sharkovsky ordering, we demonstrate that it is sufficient to consider only odd initial values when studying the iterations of the Collatz map.

Next, we introduce the concept of direction phases in the iteration trajectory. Using the cobweb diagram of the Collatz map, we decompose the iteration trajectory into up and down phases. A family of recursive functions, F_s,

is defined based on the number s of up phases, and the relationship between the number of iterations and the number of up phases is clarified. We show that, starting from an initial value $X_0 \in \mathbb{F}$, the iteration converges to the period-three orbit, with the number of iterations increasing logarithmically with respect to the initial value. This implies that the iterative times required for convergence is relatively small, and from this perspective, the Collatz map always converges to the period-three orbit after a finite number of iterations.

Additionally, the function family F_s defines the attraction domains of the Collatz map. Within a given interval, the relative sizes of the attraction domains, except for the attraction domain $p = 3m$, follow a power-law distribution. It is estimated that approximately 93.77% of odd numbers belong to the attraction domain $p = 2$, and the combined proportion of the attraction domains $p = 2, 4, 5$ is as high as 99.93%. Furthermore, when all odd numbers are classified based on the number of up phases, the number of odd numbers in each up phase approximately follows a Gamma distribution. Moreover, the Ulam spiral diagram reveals that odd numbers exhibit a rich self-similarity structure when classified by attractors.

Finally, theoretical analysis shows that, in binary representation, the Collatz map is equivalent to a shift map. Based on the ergodicity of Bernoulli shift maps, we can infer that the Collatz map will inevitably evolve to its attractor X^p after a finite number of iterations, thus confirming the validity of the Collatz conjecture.

Overall, this work enhances our understanding of one of mathematics' most puzzling problems by linking it to deep concepts in nonlinear dynamics and statistical analysis. It provides valuable insights into both the specific behavior of the Collatz map and the general behavior of complex discrete dynamical systems, as well as the study of number theory. For example, within the computational scope of this study, all odd numbers align with theoretical expectations, implying that all odd numbers studied here can be generated by F_s. It is reasonable to conjecture that all odd numbers can be written in the form of the F_s function. Therefore, investigating the properties of the function F_s may yield unexpected insights into the distribution of prime numbers, as all prime numbers (except for the smallest prime, 2, which is even) are odd and can be generated by F_s.

ACKNOWLEDGMENTS

This work was supported by the National Science Foundation of China (Grants No. 12465010, No. 12247106, No. 12005156, No. 11975190, and No. 12247101). W. Fu also acknowledge support by the Youth Talent (Team) Project of Gansu Province; the Long-yuan Youth Talents Project of Gansu Province; the Project of Fei-tian Scholars of Gansu Province; the Leading Talent Project of Tianshui City; and the Innovation Fund from Department of Education of Gansu Province (Grant No. 2023A-106).

[1] E. Ott, Strange attractors and chaotic motions of dynamical systems, Rev. Mod. Phys. **53**, 655 (1981).
[2] J. J. Kozak, M. K. Musho, and M. D. Hatlee, Chaos, periodic chaos, and the random-walk problem, Phys. Rev. Lett. **49**, 1801 (1982).
[3] F. Mogavero, N. H. Hoang, and J. Laskar, Timescales of chaos in the inner solar system: Lyapunov spectrum and quasi-integrals of motion, Phys. Rev. X **13**, 021018 (2023).
[4] D. Pazó, Discontinuous transition to chaos in a canonical random neural network, Phys. Rev. E **110**, 014201 (2024).
[5] S.-D. Börner, C. Berke, D. P. DiVincenzo, S. Trebst, and A. Altland, Classical chaos in quantum computers, Phys. Rev. Res. **6**, 033128 (2024).
[6] D. Lippolis, Thermodynamics of chaotic relaxation processes, Phys. Rev. E **110**, 024215 (2024).
[7] A. Fuchs, *Nonlinear dynamics in complex systems* (Springer, 2014).
[8] R. H. Abraham, L. Gardini, and C. Mira, *Chaos in Discrete Dynamical Systems*, 1st ed. (Springer New York, NY, 1997).
[9] H.-O. Peitgen, H. Jürgens, and D. Saupe, *Chaos and Fractals: New Frontiers of Science*, 2nd ed. (Springer, 2004).
[10] K. E. Yao and Y. Shi, Hopf bifurcation in three-dimensional based on chaos entanglement function, Chaos, Solitons & Fractals: X **4**, 100027 (2019).
[11] H. Rouah, Stability analysis and suppress chaos in the generalized lorenz model, Chaos, Solitons & Fractals: X **12**, 100104 (2024).
[12] M. J. Feigenbaum, Quantitative universality for a class of nonlinear transformations, J. Stat. Phys. **19**, 25 (1978).
[13] B. V. Chirikov, A universal instability of many-dimensional oscillator systems, Phys. Rep. **52**, 263 (1979).
[14] E. Ott, *Chaos in Dynamical Systems*, 2nd ed. (Cambridge university press, 2002).
[15] M. C. Mackey, The dynamic origin of increasing entropy, Rev. Mod. Phys. **61**, 981 (1989).
[16] D. J. Driebe, *Fully Chaotic Maps and Broken Time Symmetry*, Nonlinear Phenomena and Complex Systems, Vol. 4 (Springer Dordrecht, 1999).
[17] A. N. Šharkowskii, Co-existence of the cycles of a continuous mapping of the line into itself, Ukrain. Mat. Z. **16**, 61 (1964).
[18] P. Štefan, A theorem of šarkovskii on the existence of periodic orbits of continuous endomorphisms of the real line, Commun. Math. Phys. **54**, 237 (1977).
[19] T.-Y. Li and J. A. Yorke, Period three implies chaos, Amer. Math. Monthly **82**, 985 (1975).
[20] P. E. Kloeden, On sharkovsky's cycle coexistence order-

ing, Bull. Aust. Math. Soc. **20**, 171 (1979).
[21] C. Oestreicher, A history of chaos theory, Dialogues Clin. Neuro. **9**, 279 (2007).
[22] E. N. Lorenz, Deterministic nonperiodic flow, J. Atmos Sci. **20**, 130 (1963).
[23] I. Prigogine and I. Stengers, *The end of certainty* (Simon and Schuster, 1997).
[24] G. M. Zaslavsky, *Hamiltonian chaos and fractional dynamics* (Oxford University Press, USA, 2005).
[25] J. Gleick, *Chaos: Making a New Science* (Penguin, 2008).
[26] Y. G. Sinai, Statistical (3x + 1) problem, Commun. Pure Appl. Math. **56**, 1016 (2003).
[27] G. J. Wirsching, *The Dynamical System Generated by the 3n+1 Function*, 1st ed., Lecture Notes in Mathematics, Vol. 1681 (Springer Berlin, Heidelberg, 1998).
[28] R. E. Crandall, On the "3x +1 " problem, Math. Comput. **32**, 1281 (1978).
[29] I. Krasikov, How many numbers satisfy the 3x + 1 conjecture?, Internat. J. Math. & Math. Sci. **12**, 791 (1989).
[30] T. Tao, Almost all orbits of the collatz map attain almost bounded values (2022), arXiv:1909.03562 [math.PR].
[31] M. Einsiedler and T. Ward, *Ergodic Theory: with a view towards Number Theory*, 1st ed., Graduate Texts in Mathematics, Vol. 259 (Springer London, 2011).
[32] W. Wang, Z. Liu, and B. Hu, Phase order in chaotic maps and in coupled map lattices, Phys. Rev. Lett. **84**, 2610 (2000).
[33] B. Sriraman, ed., *Handbook of the Mathematics of the Arts and Sciences*, 1st ed. (Springer Cham, 2021) p. 151.